ACS APPLIED MATERIALS & INTERFACES

Research Article

www.acsami.org

Origin of Bias-Stress Induced Instability in Organic Thin-Film Transistors with Semiconducting Small-Molecule/Insulating Polymer Blend Channel

Ji Hoon Park,[†] Young Tack Lee,[†] Hee Sung Lee,[†] Jun Young Lee,[†] Kimoon Lee,[†,§] Gyu Baek Lee,[†,§] Jiwon Han,[‡] Tae Woong Kim,[‡] and Seongil Im*[,†]

[†]Institute of Physics and Applied Physics, Yonsei University, Seoul 120-749, Korea

[‡]Samsung Display Co., Ltd., #95 Samsung 2-ro, Giheung-gu, Yongin-si, Gyeonggi-do 446-711, Korea

Supporting Information

ABSTRACT: The stabilities of a blending type organic thin-film transistor with phase-separated TIPS-pentacene channel layer were characterized under the conditions of negative-bias-stress (NBS) and positive-bias-stress (PBS). During NBS, threshold voltage (V_{th}) shifts noticeably. NBS-imposed devices revealed interfacial trap density-of-states (DOS) at 1.56 and 1.66 eV, whereas initial device showed the DOS at only 1.56 eV, as measured by photoexcited charge-collection spectroscopy (PECCS) method. Possible origin of this newly created defect is related to ester group in PMMA, which induces some hole traps at the TIPS-pentacene/*i*-PMMA interface. PBS-imposed device showed little V_{th} shift but visible off-current increase as "back-channel" effect, which is attributed to the water molecules trapped on the TFT surface.

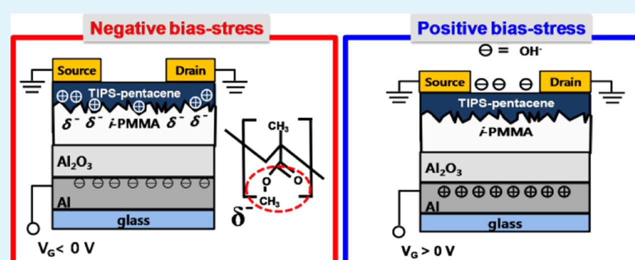

KEYWORDS: *TIPS-pentacene, blend, stability, bias-stress, photoexcited charge collection spectroscopy (PECCS), scanning kelvin probe microscopy (SKPM)*

INTRODUCTION

Organic-based electronic devices have attracted a great deal of attention over the last decades, because of their potentials in low-cost fabrication, which thus brings their research scope to solution processes utilizing small-molecule, polymer, and meta nanoparticles.[1−4] Such solution processes often include blending two materials in the prospect of gaining improved performances that single material component may not achieve without being combined with others.[5−9] When blending organic materials, several examples of organic thin-film transistors (TFTs) have been demonstrated, particularly using commercially available, 6,13-bis(triisopropylsilylethynyl)-pentacene (TIPS-pentacene) as a backbone material, since it is an active channel semiconductor of organic TFTs and has reasonable air-stability and mobility.[2,5−10] Recently, Ohe et al., Kang et al. and Hamilton et al. attempted to blend the TIPS-pentacene with poly (α-methylstyrene) (PαMS), which resulted in quite decent mobilities exceeding ~0.1 cm^2/ V s along with good performance uniformity.[6−8] We also have recently fabricated such blending (TIPS-pentacene/PMMA) type TFTs with phase-separated layers utilizing so-called "vertical flowing" technique, and reported anisotropic crystalline growth of TIPS-pentacene in the blend.[11,12] Most of the blending type organic TFTs have shown somewhat improved performance, uniformity, and reproducibility that are superior to those of sole TIPS-pentacene based TFTs.[7,9]

In spite of such improved aspects, the electrical stabilities of the blending type organic TFTs have rarely been characterized although the stabilities are maybe more important factors in practical applications which request electrical stabilities under negative and positive types of gate bias stresses.[13−22] In general, the threshold voltage (V_{th}) shift has been an important indicator of degradation in organic TFT during the stress,[16,19,21,22] and to the best of our limited knowledge, systematic bias-stress experiment and V_{th} analysis on the blending type TFT are still lacking,[17,18] although many bias-stress results have been reported with single-component based organic TFTs.[13,14,16,19−21] In the present work, we report the results from the bias-stress effects on the blending type TFTs, along with the detailed analysis results from photoexcited charge collection spectroscopy (PECCS) and scanning kelvin probe microscope (SKPM).

EXPERIMENTAL SECTION

Above all, a TIPS-pentacene/isotactic poly-(methyl methacrylate) (*i*-PMMA) blend solution (master solution) was prepared according to our previously reported research.[11,12] Then, a bottom gate electrode of 100 nm-thick Al was thermally evaporated to be patterned on glass (Eagle 2000) through a shadow mask. A 100 nm-thick AlO_x film was

Received: October 17, 2012
Accepted: February 20, 2013
Published: February 20, 2013

 © 2013 American Chemical Society

deposited by rf magnetron sputtering at room temperature (RT), and hexamethyldisilazane (HMDS) was coated by spin-coating, to be annealed at 110 ° C. The master solution was vertically flowed through pipet on the sputter-deposited AlO_x, beneath which the patterned gate (G) Al was aligned. After film-drying process for overnight in vacuum, Au source/drain (S/D) electrode were fabricated by S/D patterning through shadow masks (more details of this process are found elsewhere).[11,12] The TFT have nominal channel length (L) and width (W) of 90 and 1000 μm, respectively. All the electrical measurements such as drain current-gate voltage (I_D-V_G) transfer characteristics and gate-bias stress test were performed with Agilent 4155C semiconductor parameter analyzer in the dark and in an ambient condition of relative humidity of 40%. Photoexcited charge collection spectroscopy (PECCS) was performed with a light source (500 W, Hg(Xe) arc lamp), a gratings monochromator covering the spectral range of 254–1000 nm, and an optical fiber (core diameter of 200 μm) as an optical probe which guide photons onto the top (channel region) of the working device. Photon flux of at least 5×10^{14} cm^{-2} s^{-1} (optical power density, 0.2 mW cm^{-2}) was measured after lights passed through the optical fiber (see the Supporting Information for more details on PECCS measurement steps and analysis). Noncontact mode SKPM measurements were also implemented to evaluate the distribution of surface-potential of our organic transistors[23] by using commercial atomic force microscope (AFM; Park Systems (XE-150)) connected to external lock-in amplifier (SR830, Stanford Research Systems) in ambient condition (more details are in the Supporting Information).

■ RESULT AND DISCUSSION

A schematic cross section of TIPS-pentacene/PMMA blend organic TFT is illustrated in the left of Figure 1a. The right scheme of Figure 1a illustrates the channel film part which consists of TIPS-pentacene phase separated from PMMA in the end of blending process. When our blend type organic TFT is stressed under a negative gate bias with grounded source and drain, the threshold voltage (V_{th}) shifts toward more negative side depending on stress time. On the other hand, V_{th} shift toward positive value under a positive gate bias along with apparent change in subthreshold swing (S.S.). The V_{th} shift would be caused by interface or near-interface charges, which are probably electrons or holes trapped at/or near the organic semiconductor/dielectric interface.[14,19,22] During the gate-bias stressing, such trappings are quite possible, resultantly modifying effective V_{th} . Figure 1b represents such bias-stress effects in view of drain current-gate voltage (I_D-V_G) transfer characteristics, even though more systematic results must be separately discussed later according to the positive and negative gate bias stresses.

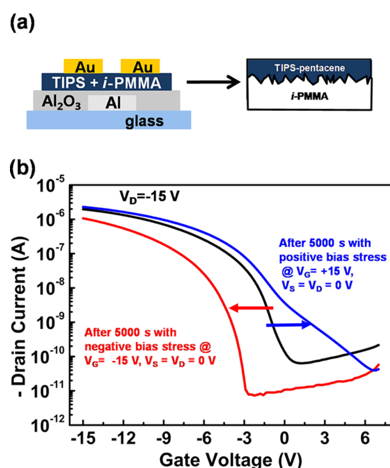

Figure 1. (a) Schematic cross section of top-contact bottom-gate TFTs we fabricated using "vertical flowing" method (left) and TIPS-pentacene/i-PMMA blend channel (right) (b) Examples of transfer characteristics showing V_{th} shift by positive- (PBS) or negative-bias-stresses (NBS) on our TIPS-pentacene/PMMA blend TFT at V_{DS} = −15 V.

When a negative bias stress (NBS) was imposed on our organic TFT with a gate bias of −15 V (ON-bias) in ambient condition for 5000 s, its stress effects on V_{th} were observed under a high drain voltage (V_D) of −15 V in Figure 2a where the curves gradually move to negative side with the stress time but without visible change of S.S. Figure 2b summarizes the time-dependent transitions of V_{th} and S.S. For 5000 s period, visible change of V_{th} was observed, to be approximately −3 V while the S.S. plot did show only a little change of S.S. from 0.87 to 0.7 V/dec Inset in Figure 2a also displays the negative shift of the capacitance–voltage ($C-V$) curve, which proves the NBS-driven shift of V_{th} with flat band voltage (V_{FB}) shift in the $C-V$ behavior.[24] These NBS results lead us to surmise that there exists difference in interfacial trap states before and after NBS test, which was really observed by PECCS measurements.[25,26]

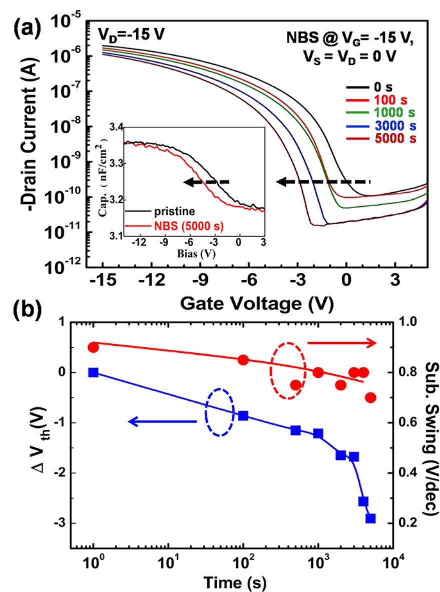

Figure 2. (a) Transfer characteristics (I_D-V_G) of blend TFT taken after time-dependent NBS at V_G of −15 V with V_S = V_D = 0 V. Inset shows $C-V$ characteristics before (black) and after (red) NBS test. (b) The plots of ΔV_{th} and S. S. vs time.

Panels a and b in Figure 3 display the photoinduced transfer curves obtained at a linear regime V_D of −0.5 V from our TIPS-pentacene/PMMA blending type TFT before (pristine) and after NBS test. The curves are necessary as an initial step to analyze the interfacial trap density-of-states (DOS), and show a photoinduced V_{th} shift toward (+) direction which is opposite to the shift shown in Figure 2a (as indicated by arrows), since photons are not charging but instead releasing the trapped holes. Although the photoinduced hole-releasing appeared not much significant with small V_{th} shift which is due to the low V_D, the hole detrapping was clear in the zoomed view of the transfer curves (insets), and the photoinduced V_{th} shift was more obvious in the NBS-stressed device. In general, when the

dx.doi.org/10.1021/am3022703 | ACS Appl. Mater. Interfaces 2013, 5, 1625−1629

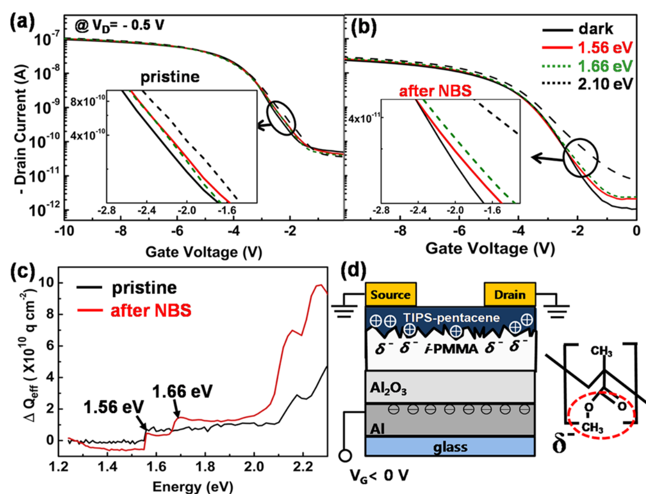

Figure 3. Photoinduced transfer curves of (a) pristine unstressed TFT and (b) negative-bias stressed TFT. Each inset shows magnified view of phototransfer curves (c) ΔQ_{eff} (ε) vs ε plot of pristine (black) and negative-bias stressed (red) TFT. (d) Schematic cross-section of our phase-separated channel of TFT which depicts trapped holes as attracted by the negatively charged ester group (δ-) at/near the TIPS-pentacene/PMMA interface.

photoexcitation begins by monochromatic photons during transfer curve measurement, the charge carriers (holes) trapped at a matched energy level are detrapped and liberated to the highest occupied molecular orbital (HOMO) edge, to be drained (please refer to our previous reports and the Supporting Information for more details on the mechanism of PECCS).[25,26] Then, positive shifts of V_{th} are monitored at some specifically matched photon-energies (i.e., 1.56 or 1.66 eV) smaller than the HOMO−LUMO (lowest unoccupied molecular orbital) gap (~2.1 eV) of TIPS-pentacene. These positive shifts of V_{th} in panels a and b in Figure 3 could be quantitatively calculated as an effective trap charge density (Q_{eff}) as plotted in Figure 3c, because $Q_{eff} = C_{ox}\Delta V_{th}$, where C_{ox} is the capacitance of PMMA/Al_2O_{3+x} double layer dielectric. Comparing the two plots performed before and after NBS, we observe apparent difference; while the two plots have a sudden increase of Q_{eff} at 1.56 eV in common, only the NBS-stressed device reveals a second Q_{eff} increase at ~1.66 eV. Although the two devices show their common increase of Q_{eff} at 1.56 and ~2.1 eV (which is regarded as the HOMO−LUMO gap), the higher interfacial Q_{eff} is certainly noticed from NBS-stressed device due to the jump at 1.66 eV, estimated to be ~5 × 10^9 q cm $^{-2}$. In fact, the number density of the detrapped charge is regarded reasonable, since it is quite the same as the trapped charge density which is now calculated in consideration of flat band voltage shift shown in the inset $C-V$ curves of Figure 2a. Integrated area between the two $C-V$ curves of the inset means the trapped charge density, which was calculated out to be ~8.8 × 10^9 q cm^{-2}. We may not clearly know the nature of the deep interfacial traps found at 1.56 and 1.66 eV, however, some speculation on the new traps at 1.66 eV is suggested; the interfacial states at 1.56 eV are related to deep-level hole traps but new interfacial states form when ester groups (δ−) with strong negative dipole (due to oxygen atoms; Figure 3d) in PMMA attract (or detain) hole carriers at the TIPS-pentacene/PMMA interface under the NBS.[27] (The ester group with negative dipole, as attached to the PMMA backbone, might be rotated to get closer to the interface under a negative gate bias.) The resulting energy level of new interfacial states is observed at 1.66 eV. This conjecture is regarded reasonable in view of Figure 2a where the off-current level gradually decreases with the NBS time; more hole charges are to be trapped at the interface by ester groups of PMMA as time elapses longer. The schematic cross section of our phase-separated channel of TFT in Figure 3d illustrates the holes being trapped by the δ− groups at/near the TIPS-pentacene/PMMA interface.

Figure 4 displays the trap DOS profiles as obtained by differentiating the effective trap charge density (Q_{eff}) plot of

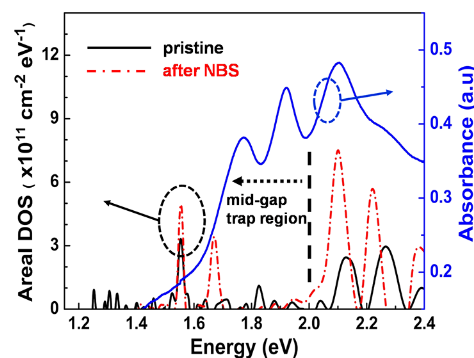

Figure 4. DOS plots for pristine and negative bias-stressed blend TFT as obtained by differentiating ΔQ_{eff} (ε) with photon energy in Figure 3c. The optical absorbance spectrum of TIPS-pentacene/PMMA on glass is overlaid to be compared with the DOS profile.

Figure 3c with photon energy. The blue curve overlaid on the trap DOS profile corresponds to optical absorption spectrum of our TIPS-pentacene/PMMA film on glass. Our trap DOS profile displays interface trap-induced peaks at 1.56 and 1.66 eV after NBS while it shows a HOMO energy level near 2.10 eV, which is ~0.35 eV larger than 1.76 eV, an optical HOMO−LUMO gap in blue curve. This energy discrepancy of ~0.35 eV is attributed to exciton binding energy in TIPS-pentacene solid. It is worthwhile to note that apparent interfacial peak at 1.66 eV is only monitored from the NBS-stressed device, and also worthy of note that our PECCS profile shows the replica of the three absorption peaks at 2.1, 2.22, and 2.38 eV. Our DOS profiles interestingly appear comparable to absorption spectra of oxidant-doped TIPS pentacene molecules, which were measured as a reference for charge modulated spectroscopy (CMS) of TIPS pentacene-based TFTs.[28]

Figure 5a displays the change of transfer curves under +15 V positive bias stress (PBS) which was imposed on our air-exposed organic TFTs with different time conditions. Even after a 5000 s-prolonged stress, only a little positive shift of V_{th} (by ~0.25 V) was observed but anomalous off-current increase was also observed unlike the case of NBS in Figure 2a. Figure 5b summarizes the V_{th} shift and S.S. change as the time-dependent plots. According to the plots, 500 s appears as a starting point of S.S. transition. The V_{th} shift almost stops around at 1000 s but significant S.S. degradation continues. Such S.S. increase is not likely to be related to accumulation charge or traps at/near the channel interface, since it has not been observed from NBS-devices. We thus suspected this type of S.S. change might come from 'back-channel' effect, which has been reported elsewhere in many type of TFTs.[29−32] Hoshino et al. systematically studied the device characteristics of moisture, and explained the possible mechanism of moisture-induced change in P3HT device characteristics.[29] If water

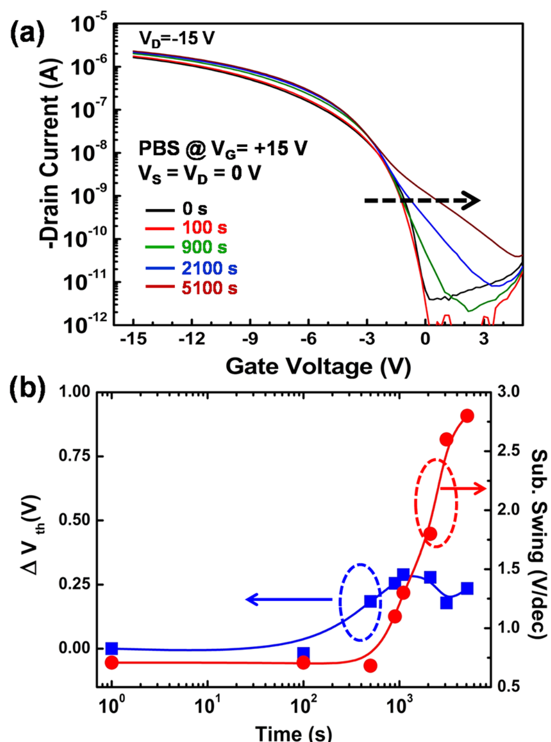

Figure 5. (a) Transfer characteristic (I_D−V_G) of our blend TFT under time-dependent PBS at V_G of +15 V with V_S = V_D = 0 V (b) The plots of ΔV_{th} and S. S. as a function of time.

molecules are absorbed on the surface of an air-exposed semiconducting layer (with bottom-gate structure), the surface induces or attracts some mobile charges and acts as an additional channel layer. These additional charges, which should be holes in our OTFT case cause the increase of off-state and even on-state current in the organic TFT devices.[32] In this regard, passivation layer is always necessary.

To ensure our speculation on PBS-driven back-channel, we implemented two types of experiments. First, we allowed the PBS-tested device for 5000 s to again go through NBS test for 1000 s. As a result, we observe that the device subsequently recovers its initial states as shown in the transfer curves of Figure 6a. Because the back-channel surface of our PBS-tested device basically contains adsorbed-water molecules or negatively charged hydroxyl-groups, it probably attracts the holes in the TIPS-pentacene film as the source of off-current increase. Under the sequential long-term NBS stress, the adsorbed molecules are detached from the surface by coulomb repulsion, recovering the device to its initial states. The "back-channel" effect was again confirmed by scanning kelvin probe microscopy (SKPM) measurement which was directly conducted on our TFT under a positive bias condition: +10 V of V_G and V_S = V_D = 0 V (see the inset of Figure 6a for the SKPM measurement scheme on the positively gate-biased device, in which the depletion width of TIPS-pentacene would be almost the same as the semiconductor film thickness itself; our TIPS-pentacene/PMMA blend film has its thickness of ~450 nm as a whole but respective thicknesses were 250/200 nm[12]). As shown in the two-dimension potential topography image of Figure 6b, negative potential was by and large detected from the TIPS-pentacene surface under the V_G of +10 V. It is thus likely that adsorbed H_2O molecule on the organic semiconductor film surface may be dissociated into H^+ and OH^- moieties under the applied V_G. (H ions now become gas phase and remaining OH− groups show negative potentials under SKPM probe).

SUMMARY

The stabilities of a blending type organic TFT with phase-separated TIPS-pentacene channel layer were characterized under the conditions of NBS and PBS. NBS-taken devices revealed interfacial trap DOS at 1.56 and 1.66 eV, whereas unstressed device showed the DOS at only 1.56 eV, as measured by PECCS method. Possible origin of this newly created defect is related to ester group in PMMA, which induces some hole traps at the TIPS-pentacene/*i*-PMMA interface. When the device has no passivation layer, PBS induces "back-channel" effect, attracting the water molecules to be trapped on the TFT surface beneath, which some holes could be released causing off-current increase.

ASSOCIATED CONTENT

Supporting Information

Details on experimental theory and setup on PECCS characterization and SKPM measurement. This material is available free of charge via the Internet at http://pubs.acs.org.

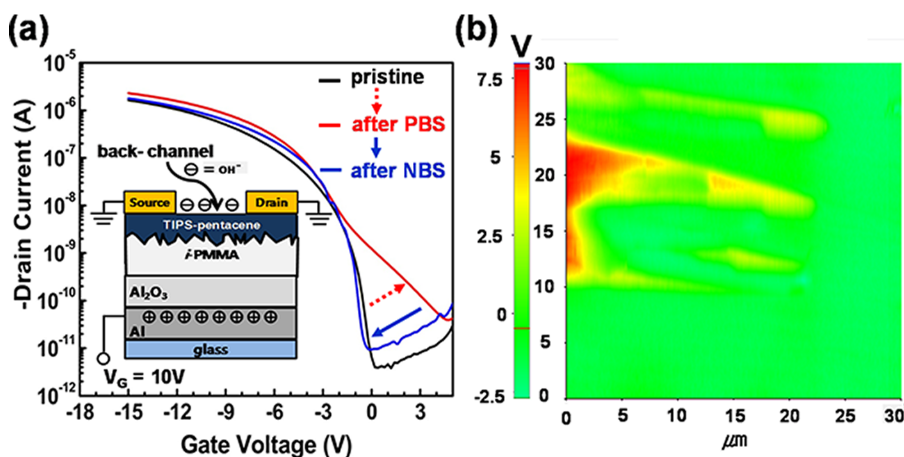

Figure 6. (a) Transfer characteristics of pristine, PBS, and consecutive NBS-imposed TFTs. Inset shows schematic cross-section of PBS-tested TFT with the molecule (OH−)-adsorbed surface as back-channel, (b) of which the potential was mapped by SKPM at V_G of +10 V.

dx.doi.org/10.1021/am3022703 | ACS Appl. Mater. Interfaces 2013, 5, 1625−1629

AUTHOR INFORMATION

Corresponding Author

*TEL: +82-2-2123-2842. FAX: +82-2-392-1592. E-mail: semicon@yonsei.ac.kr.

Present Address

§K. Lee is currently with Frontier Research Center, Tokyo Institute of Technology in Japan and G. Lee is working at Park SYSTEMS in Korea.

Notes

The authors declare no competing financial interest.

ACKNOWLEDGMENTS

The authors acknowledge the financial support from KOSEF (NRL program, 2012-0000126), and Brain Korea 21 Project.

REFERENCES

(1) Halik, M.; Klauk, H.; Zschieschang, U.; Schmid, G.; Dehm, C.; Schutz, M.; Maisch, S.; Effenberger, F.; Brunnbauer, M.; Stellacci, F. *Nature* **2004**, *431*, 963−966.
(2) Lim, J. A.; Lee, H. S.; Lee, W. H.; Cho, K. *Adv. Funct. Mater.* **2008**, *19*, 1515−1525.
(3) Yan, H.; Chen, Z.; Zheng, Y.; Newman, C.; Quinn, J. R.; Dötz, F.; Kastler, M.; Facchetti, A. *Nature* **2009**, *457*, 679−686.
(4) Chung, S.; Lee, J.; Song, H.; Kim, S.; Jeong, J.; Hong, Y. *Appl. Phys. Lett.* **2011**, *98*, 153110.
(5) Hwang, D. K.; Fuentes-Hernandez, C.; Berrigan, J.; Fang, Y.; Kim, J.; Potscavage, W.; Cheun, H.; Sandhage, K.; Kippelen, B. *J. Mater. Chem.* **2012**, *22*, 5531−5537.
(6) Ohe, T.; Kuribayashi, M.; Yasuda, R.; Tsuboi, A.; Nomoto, K.; Satori, K.; Itabashi, M.; Kasahara, J. *Appl. Phys. Lett.* **2008**, *93*, 053303.
(7) Kang, J.; Shin, N.; Jang, D. Y.; Prabhu, V. M.; Yoon, D. Y. *J. Am. Chem. Soc.* **2008**, *130*, 12273−12275.
(8) Hamilton, R.; Smith, J.; Ogier, S.; Heeney, M.; Anthony, A. E.; McCulloch, I.; Veres, J.; Bradley, D. D. C.; Anthopoulos, T. D. *Adv. Mater.* **2009**, *21*, 1166−1171.
(9) James, D.; Charlotte Kjellander, B. K.; Smaal, W. T. T.; Gelinck, G.; Combe, C.; McCulloch, I.; Wilson, R.; Burroughes, J.; Bradley, D. D. C.; Kim, J. *ACS Nano* **2011**, *5*, 9824−9835.
(10) Choi, D.; Ahn, B.; Kim, S. H.; Hong, K.; Ree, M.; Park, C. E. *ACS Appl. Mater. Interfaces* **2012**, *4*, 117−122.
(11) Park, J. H.; Lee, K. H.; Mun, S.-J.; Ko, G.; Heo, S. J.; Kim, J. H.; Kim, E.; Im, S. *Org. Electron.* **2010**, *11*, 1688−1692.
(12) Park, J. H.; Lim, H.; Cheong, H.; Lee, K. M.; Sohn, H. C.; Lee, G.; Im, S. *Org. Electron.* **2012**, *13*, 1250−1254.
(13) Lee, J.; Kim, D. H.; Lee, B.-L.; Park, J.-I.; Yoo, B.; Kim, J. Y.; Moon, H.; Koo, B.; Jin, Y.-W.; Lee, S. *J. Appl. Phys.* **2011**, *110*, 084511.
(14) Zilker, S. J.; Detcheverry, C.; Cantatore, E.; de Leeuw, D. M. *Appl. Phys. Lett.* **2001**, *79*, 1124.
(15) Street, R. A.; Salleo, A.; Chabinyc, M. L. *Phys. Rev. B.* **2003**, *68*, 085316.
(16) Choi, H. H.; Lee, W. H.; Cho, K. *Adv. Funct. Mater.* **2012**, *22*, 4833−4839.
(17) Kim, Y.; Anthony, J. E.; Park, S. K. *Org. Electron.* **2012**, *13*, 1152−1157.
(18) Lee, W. H.; Kwak, D.; Anthony, J. E.; Lee, H. S.; Choi, H. H.; Kim, D. H.; Lee, S. G.; Cho, K. *Adv. Funct. Mater.* **2012**, *22*, 267−281.
(19) Sirringhaus, H. *Adv. Mater.* **2009**, *21*, 3859−3873.
(20) Kalb, W. L.; Mathis, T.; Haas, S.; Stassen, A. F.; Batlogg, B. *Appl. Phys. Lett.* **2007**, *90*, 092104.
(21) de Leeuw, D. M.; Simenon, M. M. J.; Brown, A. R.; Einerhand, R. E. F. *Synth. Met.* **1997**, *87*, 53−59.
(22) Kim, D. H.; Lee, B.; Moon, H.; Kang, H. M.; Jeong, E. J.; Park, J.; Han, K.; Lee, S.; Yoo, B. W.; Koo, B. W.; Kim, J. Y.; Lee, W. H.; Cho, K.; Becerril, H. A.; Bao, Z. *J. Am. Chem. Soc.* **2009**, *131*, 6124−6132.
(23) Tello, M.; Chiesa, M.; Duffy, C. M.; Sirringhaus, H. *Adv. Funct. Mater.* **2008**, *18*, 3907−3913.
(24) Sze, S. M.; *Physics of Semiconductor Devices*, 2nd ed.; Wiley: New York, 1981; Chapter 7, pp 362−430.
(25) Lee, K.; Oh, M. S.; Mun, S.; Lee, K. H.; Ha, T. W.; Kim, J. H.; Park, S.; Hwang, C.; Lee, B. H.; Sung, M. M.; Im, S. *Adv. Mater.* **2010**, *22*, 3260−3265.
(26) Lee, K.; Lee, B. H.; Lee, K. H.; Park, J. H.; Sung, M. M.; Im, S. *J. Mater. Chem.* **2010**, *20*, 2659−2663.
(27) Lee, J.; Jung, J. Y.; Kim, D. H.; Kim, J.; Lee, B.; Park, J.; Chung, J. W.; Park, J. S.; Koo, B.; Jin, Y. W.; Lee, S. *Appl. Phys. Lett.* **2012**, *100*, 083302.
(28) Sakanoue, T.; Sirringhaus, H. *Nat. Mater.* **2010**, *9*, 736−740.
(29) Hoshino, S.; Yoshida, M.; Uemura, S.; Kodzasa, T.; Takada, N.; Kamata, T.; Yase, K. *J. Appl. Phys.* **2004**, *95*, 5088−5093.
(30) Kim, Y.; Kim, H. S.; Han, J.; Park, S. K. *Appl. Phys. Lett.* **2010**, *97*, 092105.
(31) Chung, W.; Chang, T.; Li, H.; Chen, Chi.; Chen, Y.; Chen, S.; Tseng, T.; Tai, Y. *Electrochem. Solid-State Lett.* **2011**, *14*, H114−H116.
(32) Salleo, A.; Chabinyc, M. L. *Organic Electronics Materials: Manufacturing and Applications*; Klauk, H., Ed.; Wiley−VCH: Weinheim, Germany, 2006; Chapter 5, p 126.